

# TOMOGRAPHIC AND MECHANICAL STUDY OF 3D PRINTED POROUS POLYMER STRUCTURE UNDER COMPRESSION

GIANPAOLO PILLON<sup>a,b,\*</sup>, RADOSŁAW GRABIEC<sup>b</sup>, JACEK TARASIUK<sup>b</sup>,  
SEBASTIAN WRONSKI<sup>b</sup>, ANNE SOPHIE BONNET<sup>a</sup>

<sup>a</sup> *Université de Lorraine, Laboratoire d'étude LEM3 UMR CNRS 7239, 7 rue Félix Savart, 57 070 Metz, France*

<sup>b</sup> *AGH University, Faculty of Physics and Condensed Matter, Władysława Reymonta 19, 30-059 Kraków, Poland*

\* corresponding author: gianpaolo-pillon@orange.fr

**ABSTRACT.** This study investigates the influence of open porosity rate and trabeculae diameter on the compressive behavior of structure printed by DLP technology. Three types of structures have been studied : two periodic structures (Cubic and Octet) and one aperiodic structure (Voronoi-based). Each of these structures are printed with a porosity of 40, 60 and 80 % and also with two different trabeculae diameters: 0.45 mm and 0.66 mm. We investigated porosity by micro-tomography with ImageJ for the data treatment. We determined the curing time by making a compressive test for different lengths of UV cure. The first results of the study show that Cubic structure has better Young's Modulus and also better mechanical stress than Octet and Voronoi-based structures.

**KEYWORDS:** Porous structure, DLP technology, compression test, tomography, porosity, trabeculae.

## 1. INTRODUCTION

Facing the Earth's aging population, there is more and more the need to perform bone to bone transplantation. However, this method has several problems: donor compatibility, infection, disease or in the worse case, transplantation rejection. To face this problem, surgeons have been using artificial bones made of titanium or stainless steel. These structures are presenting a too vigorous Young's Modulus that lead to the stress shielding phenomenon around the artificial bone (reduction of the bone density around the prosthesis). Porous structures are good candidates because they own a lower Young's Modulus and their design allows muscle regrowth inside the prosthesis. The goal of this paper is to investigate the influence of porosity and trabeculae diameter (TD) on the mechanical properties of 3D printed porous structures. For this, Cubic, Octet and Voronoi structures are studied under compression, each structure will be studied under 3 porosity rates (40, 60 and 80 %) and each porosity is studied with two different trabeculae diameter (TD) (0.45 mm and 0.66 mm).

## 2. MATERIALS AND METHODS

### 2.1. MATERIALS

The printer used in this investigation is a Digital Light Processing (DLP) Printer Photon from the Anycubic brand (Shenzhen, Guangdong, China). DLP Technology uses the photo-sensibility of the resin to print the structure and the resin used is the Basic resin from Anycubic with a wavelength of 405 nm. The UV curing machine is an Anycubic Wash and Cure 3. The volumic image is obtained by using a Nanotom (Waygate Technologies, Pennsylvania, USA). The data are treated using the software Image J Fiji (Schindelin,

Arganda-Carreras, Cardona, Longair, Schmid, version 1.48, LOCI, University of Wisconsin) to extract the porosity as well as the trabeculae thickness. The compressive test are carried out using a Deben micro-compressive machine with a cell capacity of 5 kN and a strain rate of  $0.33 \cdot 10^{-3} \text{ s}^{-1}$  which corresponds to a compressive speed of  $0.2 \text{ mm min}^{-1}$ . The results presented in this article are an average of 5 compressive tests to have better statistical data.

### 2.2. STRUCTURE GENERATION

The structures studied in this paper are generated by coding [1]. Three types of structures are studied: Cubic and Octet structures (Figure 1) and the Voronoi structure (Figure 2).

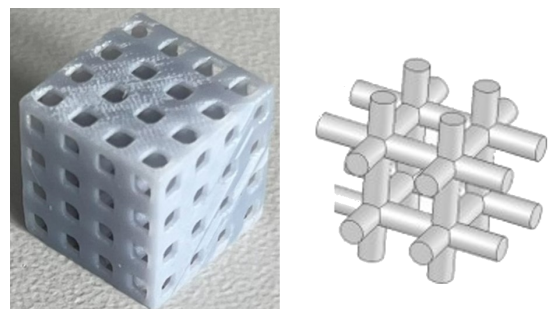


FIGURE 1. Cubic structure and its original cell [2].

These structures have a different original cell. The angle between the trabeculae is  $90^\circ$  for the Cubic structure but only  $60^\circ$  for the Octet structure. The third structure studied is a Voronoi structure based on the Voronoi diagram [1] (Figure 3). Its particularity is that the structure is randomly generated and each time the distribution is different. Three random versions of Voronoi structure have been printed

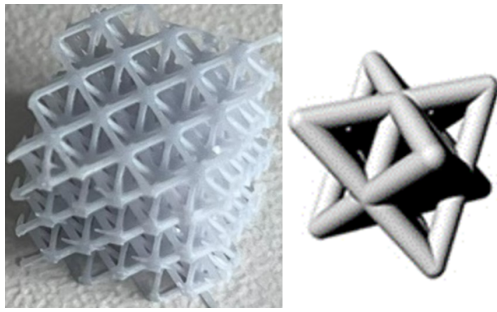


FIGURE 2. Octet structure and its original cell.

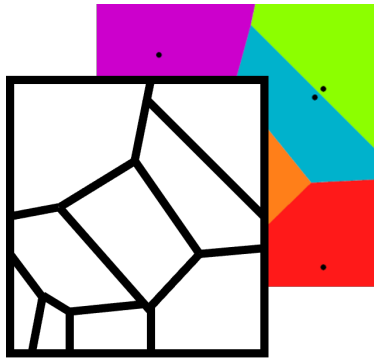


FIGURE 3. Voronoi diagram and the Voronoi network extracted from it (in black and white).

and tested to investigate the influence of randomly generated points on the mechanical behavior.

### 3. PRELIMINARY STUDY

The preliminary study was necessary in order to find the best printing parameters: the layer thickness (LT: height of the layer cure for one step), the normal exposure time (NET, amount of time one layer is exposed to UV light) and internal parameters such as porosity and TD. There is also a need to find the best curing time. Different structures were printed presenting different internal parameters. Porosity and printing defects such as layer non bonding or unwanted photo polymerization were measured by visual or by micro-tomography analysis. The Figure 4 presents a few results.

The Figure 4.1 is a Cubic structure printed with a LT of 0.8mm and a NET of 10s. The problem encountered is that free space is filled with liquid resin even after a series of washing. As the sample is cured, the liquid resin is hardened. Hence, the sample presents a porosity of 6% instead of the 60% desired. The Figure 4.2 is a Voronoi structure with the following printing parameters LT: 0.08mm and a NET: 10s. The phenomenon is the non bonding of the different layers between them. Such a problem is either because of a wide LT or a short NET. When the printing plate is going up and down, the next cured layer isn't radiated enough to stick to the previous one. The last defect is as shown on the Figure 4.3 and it is the non printing of supports or corners which

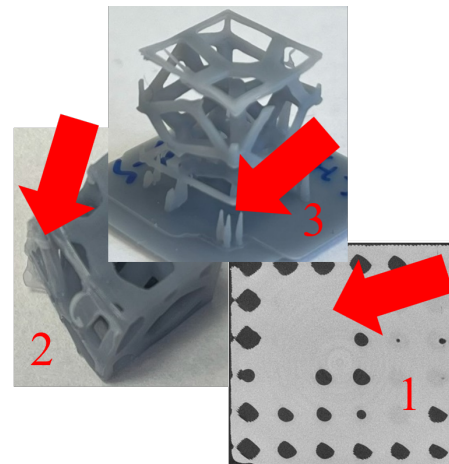


FIGURE 4. Printing defaults.

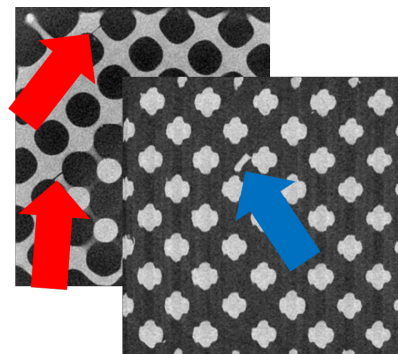


FIGURE 5. Cracks and additional parts.

ends up by affecting porosity measurements and even the mechanical behavior.

The Figures 5 are extracted from a tomography scan and two issues are appearing. The first one is the apparition of cracks after the printing and curing process. The cracks could be from the residual stress of the printing process [3]. The amount of residual stress originates from the degree of conversion of the resin and therefore from the amount of UV-light received by the resin. Such cracks have an influence on the compressive behavior because they weaken the structure. The other issue observed is the supplementary part from the previous prints 5 (blue arrow). To avoid this, the resin is frequently filtered (at least twice a week). The printing parameters chosen are LT: 0.05 mm, NET: 10 s. The internal parameters are 40, 60 and 80% with a TD of 0.45 mm or 0.66 mm.

Knowing the printing and intern parameters, the right amount of curing time can be determined by making a compressive test for different curing time (respectively 0, 3, 6, 9, 12, 15, 30 and 45 min). The more curing time there is, the more the cross linking density there is and the stronger the mechanical properties are. The chosen approach is to find the shortest curing time with best mechanical properties. Figure 6 shows the influence and the evolution of the Young's Modulus in function of the curing time.

Concerning the compressive behavior of the struc-

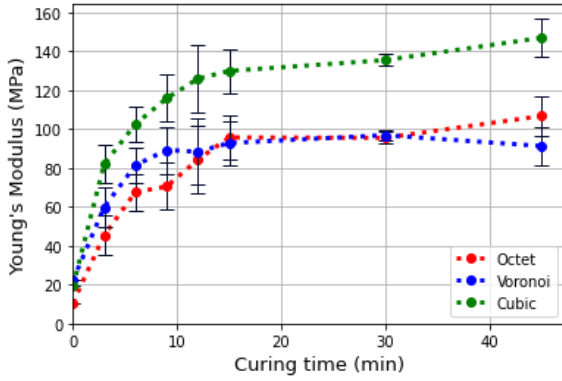


FIGURE 6. Influence of curing time on the Young's Modulus.

ture, there is clearly a limit of the Young's Modulus in function of the curing time. It is also evident that all Young's Modulus' structures have a similar behavior. However, for Octet and Cubic structures, the samples cured within 9 min or more do not follow the "right" behavior. After investigations, the Cubic samples and the Octet (only 3 min and 6 min of curing time) were printed with a bottle of resin opened in 2020 while the rest was printed with a bottle opened in 2024. Therefore there are aging consequences after the bottles are opened and similar results are observed by [4, 5] in her study. These curves are easily modeled by the equation

$$E(t) = A \left( 1 + e^{-\frac{t}{\tau}} \right) + B \quad (1)$$

with  $t$  the time variable (min) and  $A$ ,  $B$ ,  $\tau$  positive constants values. The results are gathered in the Table 1.

Narrow table	A [MPa]	B [MPa]	$\tau$ [min]
Cubic	117.41	20.96	4.95
Octet	90.75	11.80	7.01
Voronoi	68.47	21.47	3.23

TABLE 1. Values of constants.

It is well known that  $3\tau$  will give 95% of the final value (the "final" Young's Modulus) while  $5\tau$  will be for 99% of the final value. Facing the challenge with the difference of opening time of the resin, the curing time is set at 20 minutes for all structures.

To conclude the preliminary study, the printing parameters are: LT of 0.05 mm and NET of 10 s. The internal parameters are: 40, 60 and 80%, with both TD, one of 0.45 mm and one of 0.66 mm. The curing time is set at 20 min.

#### 4. RESULTS AND DISCUSSIONS

For a better comprehension of the reader, the structures are named: O\_40\_66, the letter indicates the type of structure: V for Voronoi, O for Octet and C

for Cubic. The first number indicates the porosity and the second number the trabeculae thickness (0.45 mm or 0.66 mm). There is the version but only for Voronoi structure (V1, V2 or V3).

A result of the generation of Voronoi structure, is the difference of distribution of the point and therefore, the difference of the trabeculae thickness among the structure. Since the internal structure of Voronoi version is not the same, the mechanical properties could be affected. This influence is visible on the result presented in Figure 7. The graph is the evolution of the Young's modulus regarding the porosity and also the version of Voronoi.

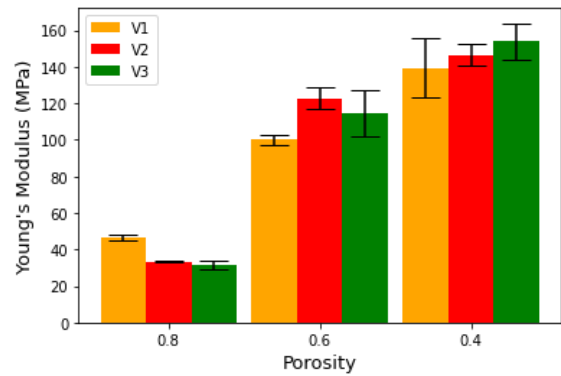


FIGURE 7. Influence of the Voronoi version on the Young's Modulus.

The Young's Modulus are diverging following the version. This result could be explained by the difference of the trabeculae thickness investigated by a tomography scan. The results are show in Figure 8.

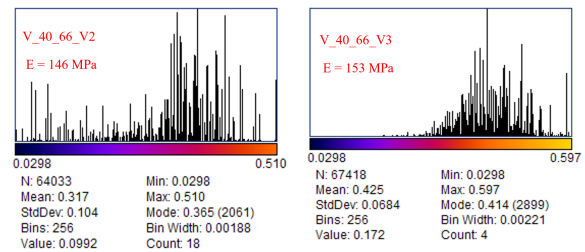


FIGURE 8. Trabeculae thickness for Voronoi versions V2 and V3.

V1 and V2 have a similar histogram of the trabeculae thickness. Structures presenting the weakest Young's Modulus are the one with the most spread trabeculae thickness (Figure 8), V2 in this case and also V1 by extension. The version V3 that has the highest elastic modulus has also the less dispersed and longest trabeculae thickness. This could explained the difference of Young's Modulus (Figure 8, V\_40\_66\_V3).

The Young's Modulus of the resin is obtained by doing an average of 5 compressive tests on a bulk cube of 10 mm side cured for 20 min. These results are an average of the Voronoi versions. According to Figure 9 the evolution of the porosity is similar for all structures.

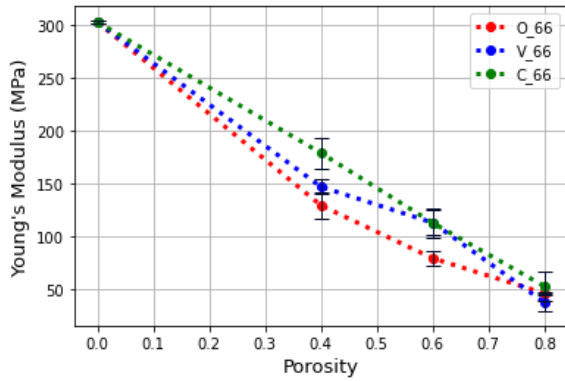


FIGURE 9. Influence of porosity for the 3 different structures.

The evolution is pseudo linear. The Voronoi sample and the Cubic sample presenting both 60% of porosity have a similar Young's Modulus (respectively 112.57 MPa and 112.40 MPa). It is also interesting to see that these samples have the same Young's Modulus as the Octet sample with 40% of porosity (129 MPa). The compressive curves of Voronoi structure are shown in Figure 10.

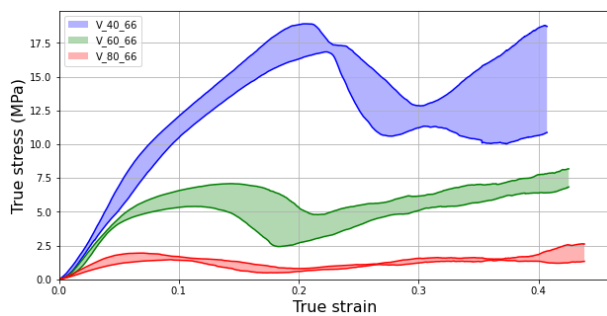


FIGURE 10. Compressive curve of Voronoi sample with different porosity.

It is clear to see that the sample with 40% of porosity has a better mechanical stress (18 MPa) compared to the other sample with a different porosity (6 MPa and 2 MPa). Although these differences, the samples with 40% and 60% are experiencing general densification after the stress drop.

Similar results are observed for the compressive test of Octet samples (Figure 11). The sample with 40% of porosity has the best mechanical behavior. However, the sample with 60% experienced a floor collapsing phenomenon. This effect is well known and it has been observed by [6] on 3D printed Triply Periodic Minimal Surface structures.

The sample with 80% of porosity is also experiencing the floor collapsing. It is easy to see the periodic increase and decrease corresponding to each floor collapsing (Figure 12). However, compared to the sample O\_60\_66 the sample C\_60\_66 has no direct densification after the stress drop.

As said in the introduction the structure will be studied with different porosity and also different TD.

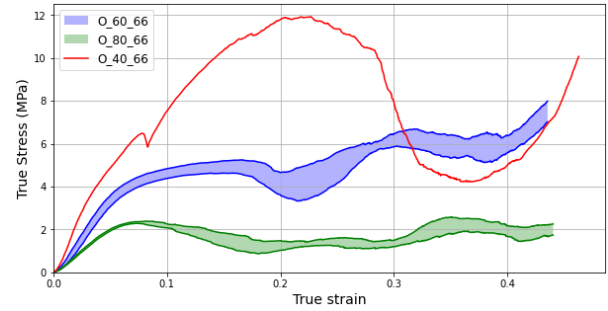


FIGURE 11. Compressive curve of Octet sample with different porosity.

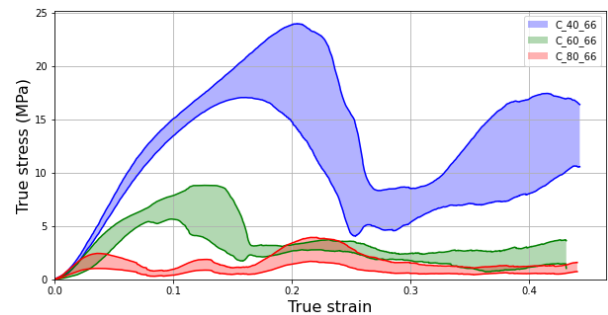


FIGURE 12. Compressive curve of Cubic sample with different porosity.

To ensure that by changing the TD, the porosity remains the same, it is necessary to add more trabecule [7].

Figure 13 shows the compressive behavior of the Voronoi sample with a porosity of 40% and two TD differences. These samples have the same Young's Modulus (respectively 138.49 MPa for 0.45 mm and 146.6 MPa for 0.66 mm). Therefore, the reduction of the diameter of the trabeculae and the increase of their number lead to similar results. The elastic parts are similar even though the sample with a TD of 0.45 mm admits more standard deviation than the other TD. There are two plastic stages, the first one starts around a strain of 0.7 and the second one starts at 0.2 of strain for both samples. This equivalence is also occurring for Octet samples with 60% of porosity (Figure 14).

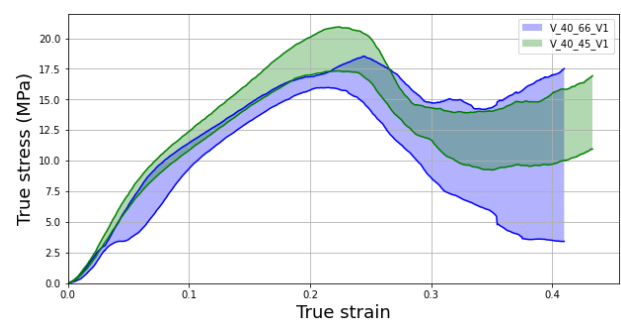


FIGURE 13. Compressive curve of V\_40\_66\_V1 and V\_40\_45\_V1.



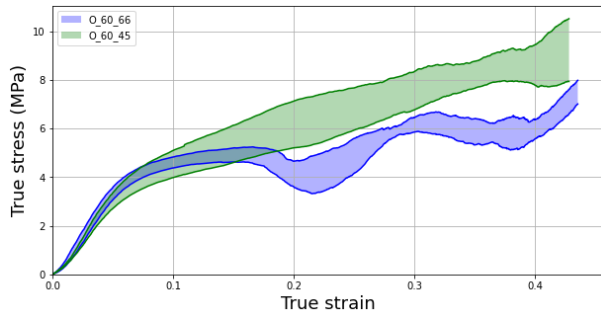


FIGURE 14. Compression curve for Octet structure presenting a different TD.

It is obvious to see both Octet structures have the same elastic behavior under compression load and the same Young's Modulus. The only slight difference is that the sample presenting a TD of 0.45 mm has a better mechanical stress than the sample with 0.66 mm (Figure 14). While for the Voronoi sample the behavior is similar even in the plastic domain, it is quite different for the Octet sample presenting 60 % of porosity. Indeed, they have a similar Young's modulus but their compressive behavior is totally different. The Figure 14 is highlighting this. The elastic and the first plastic stage are similar with both samples presenting a TD difference. The sample O\_60\_66 experiences a floor by floor while the sample O\_60\_45 has a direct general densification (Figure 14).

Another goal of the study was to compare the different structures (Cubic, Octet and Voronoi). The differences are shown below (Figure 15).

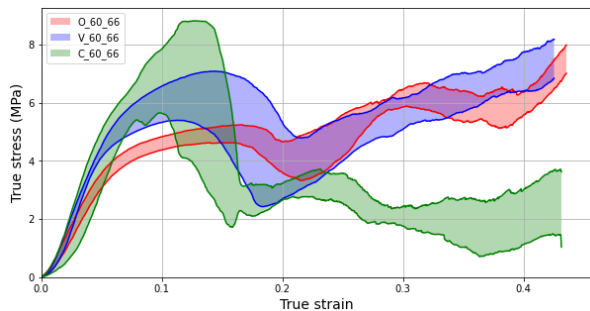


FIGURE 15. Compressive curve the different structures with 60 % of porosity.

The structures show the same behavior for the elastic zone, however, the Octet structure has a weaker mechanical stress compared to the other structure. Then, both Voronoi and Octet structures experience general densification after their smooth stress drop while the Cubic structure has a brutal stress drop and no general densification right away.

For samples presenting 80 % of porosity (Figure 16), their compressive behavior is totally different. The Cubic sample is experiencing as said previously a floor by floor densification like the Octet sample but it is less obvious. The Voronoi sample has a general densification after the stress drop.

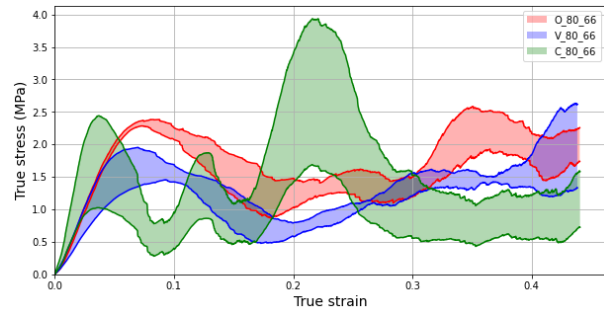


FIGURE 16. Compressive curve the different structures with 80% of porosity.

## 5. CONCLUSIONS

This article shed the light on the influence of the porosity on the mechanical behavior of 3D printed porous structure. A preliminary study was necessary to obtain all parameters and the right curing time. The influence of the random distribution for Voronoi samples was studied. Octet and Voronoi structures for specific porosity have the same elastic stage. The main differences are in the plastic response, Cubic structure tends to not experience general densification as Octet and Voronoi do so. Then, for the same structure presenting a trabeculae diameter different, the elastic stage is the same but the plastic stage is again totally different and specially for Octet structure.

## ACKNOWLEDGEMENTS

This publication was supported by the Université de Lorraine through the research Club ORION Mat & Met.

## REFERENCES

- [1] A. Tamayol, K. W. Wong, M. Bahrami. Effects of microstructure on flow properties of fibrous porous media at moderate reynolds number. *Physical Review E* **85**(2):026318, 2012. <https://doi.org/10.1103/physreve.85.026318>
- [2] R. Grabiec, J. Tarasiuk, S. Wroński. Desing of the algorithm, print and analysis of porous structures with modifiable parameters. *Acta Polytechnica CTU Proceedings* **42**:27–31, 2023. <https://doi.org/10.14311/app.2023.42.0027>
- [3] D. Xie, F. Lv, Y. Yang, et al. A review on distortion and residual stress in additive manufacturing. *Chinese Journal of Mechanical Engineering: Additive Manufacturing Frontiers* **1**(3):100039, 2022. <https://doi.org/10.1016/j.cjmeam.2022.100039>
- [4] V. Drechslerová, J. Falta, T. Fíla, et al. Effect of aging on mechanical properties of 3D printed samples using stereolitography. *Acta Polytechnica CTU Proceedings* **42**:1–5, 2023. <https://doi.org/10.14311/app.2023.42.0001>
- [5] V. Drechslerová, N. Krčmářová, J. Falta, T. Fíla. Ageing effects on the mechanical properties stability of 3D printed material under compression. *Acta Polytechnica CTU Proceedings* **48**:15–21, 2024. <https://doi.org/10.14311/APP.2024.48.0015>

- [6] M. Saleh, S. Anwar, A. M. Al-Ahmari, A. Alfaify. Compression performance and failure analysis of 3D-printed carbon fiber/PLA composite TPMS lattice structures. *Polymers* **14**(21):4595, 2022. <https://doi.org/10.3390/polym14214595>
- [7] R. Grabiec, J. Tarasiuk, S. Wroński, G. Pillon. Comparison of elastic properties of periodic and aperiodic porous structures produced by additive methods. *Acta Polytechnica CTU Proceedings* **48**:27–33, 2024. <https://doi.org/10.14311/APP.2024.48.002>